Electronic Supplementary Material (ESI) for Journal of Materials Chemistry A.

Supplementary Information

Efficacious multifunction codoping strategy on the room-temperature solution-processed hole transport layer for realizing high-performance perovskite solar cells

Dan Ouyang, Jiawei Zheng, Zhanfeng Huang, Lu Zhu, and Wallace C. H. Choy*

Department of Electrical and Electronic Engineering, The University of Hong Kong, Pokfulam Road, Hong Kong 999077, China
E-mail: chchoy@eee.hku.hk

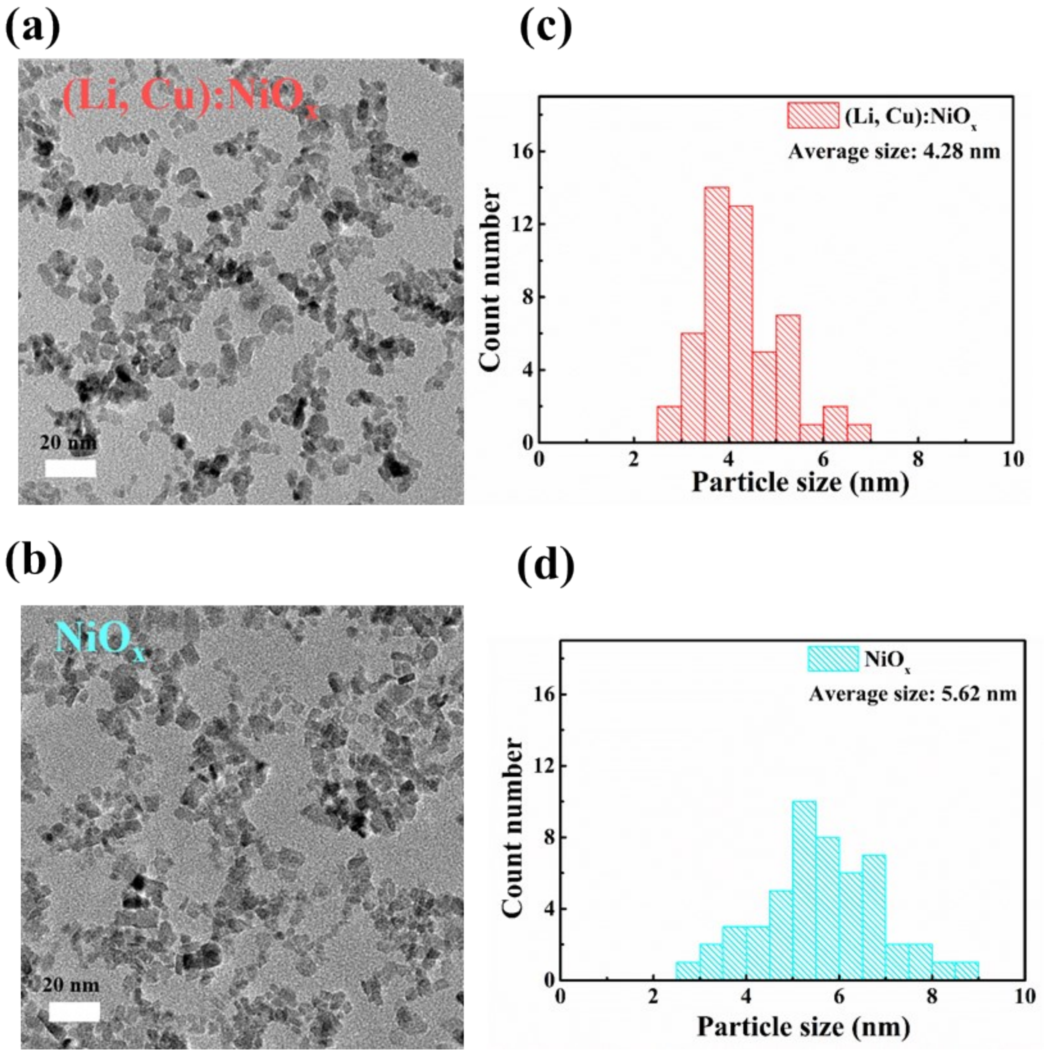

Fig. S1 TEM image of as-synthesized (a) (Li,Cu):NiO_x NPs and (b) pristine NiO_x and. Size distribution of (c) (Li, Cu):NiO_x and (d) pristine NiO_x NPs.

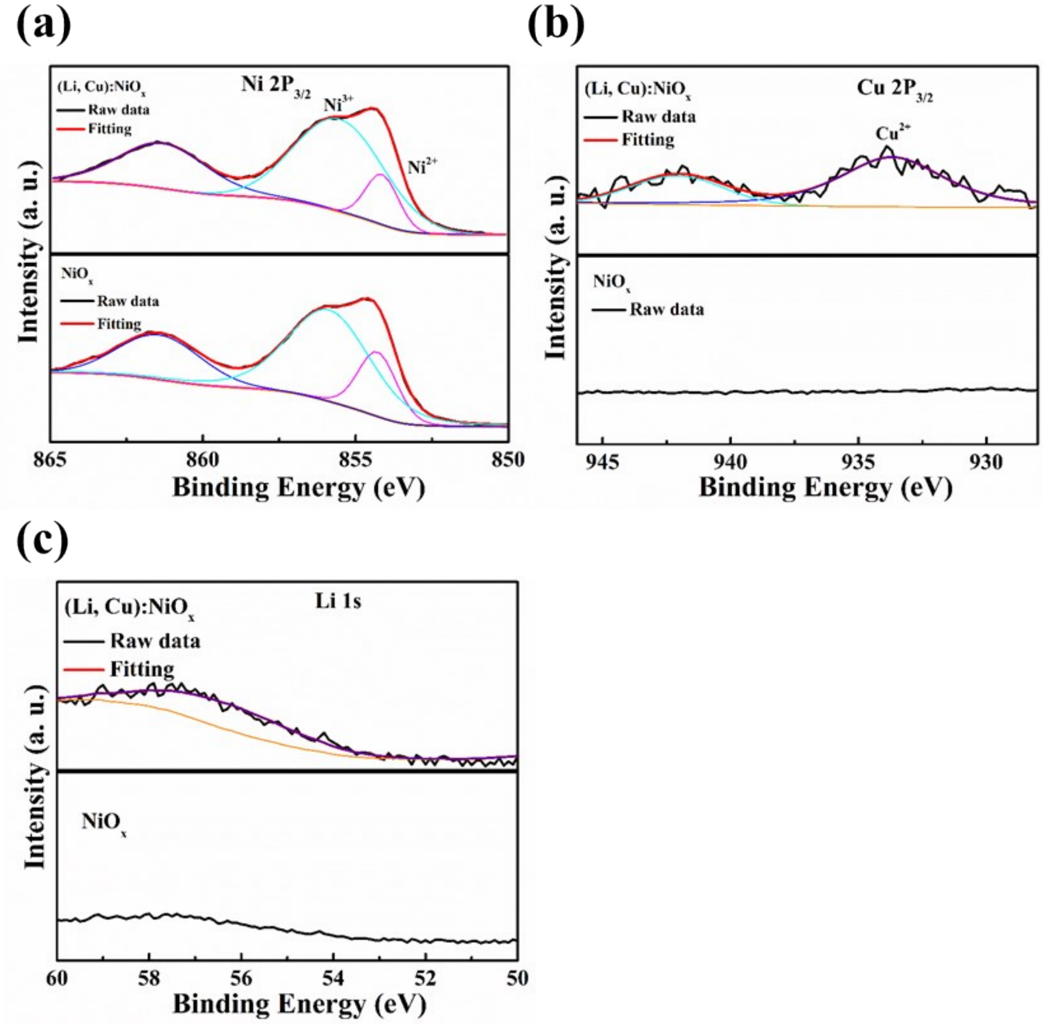

Fig. S2 High-resolution XPS spectra of (a) Ni $2p_{3/2}$, (b) Cu $2p_{3/2}$ and (c) Li 1s elements for NiO_x and (Li,Cu):NiO_x NPs.

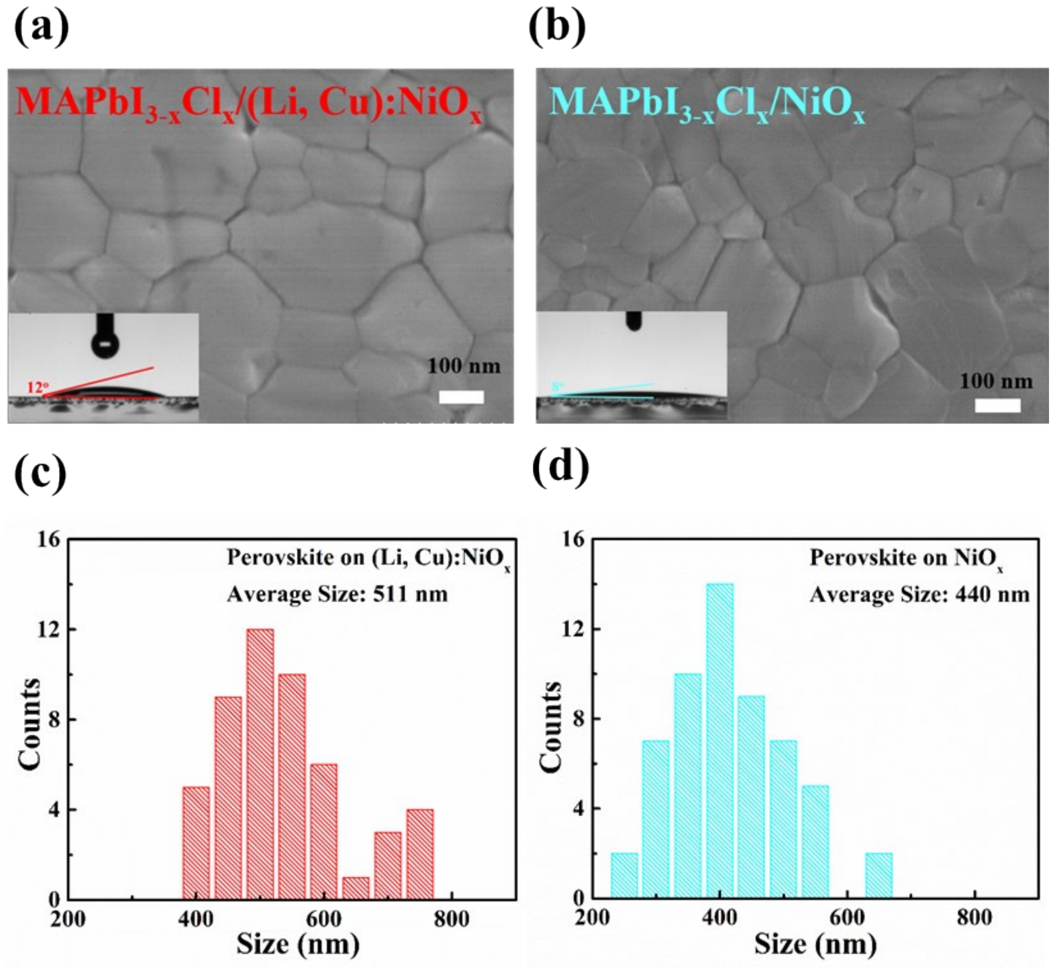

Fig. S3 SEM images of the perovskite film on (a) (Li,Cu):NiO_x, and (b) NiO_x films on ITO glass. Inserting is contact angle images of (Li,Cu):NiO_x, and NiO_x films, respectively. Size distribution of perovskite crystals on (c) (Li,Cu):NiO_x and (d) pristine NiO_x NPs, respectively.

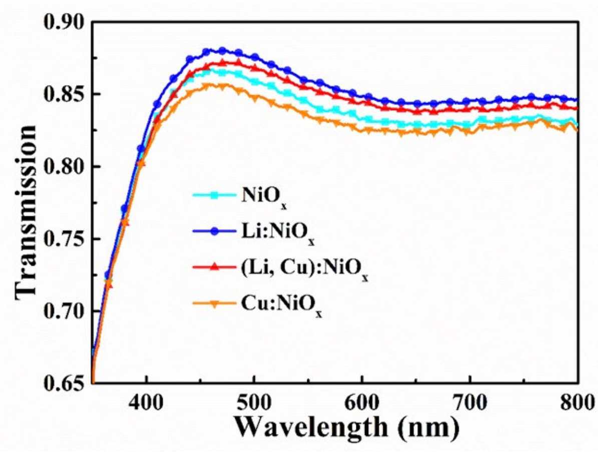

Fig. S4 Transmittance spectra of pristine NiO_x, Li:NiO_x, (Li,Cu):NiO_x, and Cu:NiO_x films on ITO glass.

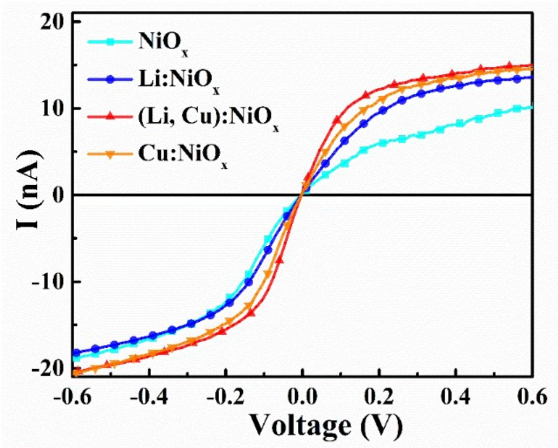

Fig. S5 I-V conducting curves of pristine NiO_x, Li:NiO_x, (Li,Cu):NiO_x, and Cu:NiO_x films measured from the c-AFM mode.

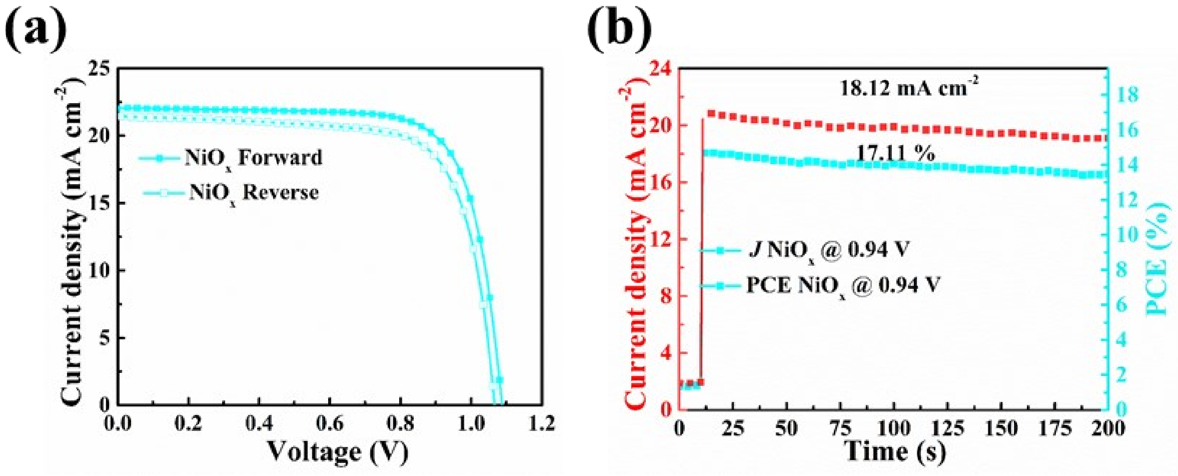

Fig. S6 (a) *J-V* characteristics of the best NiO_x based PSCs extracted from forward and reverse sweeping. (b) Steady photocurrent (red) and PCE (blue) under 1 Sun illumination of the best NiO_x based PSCs.

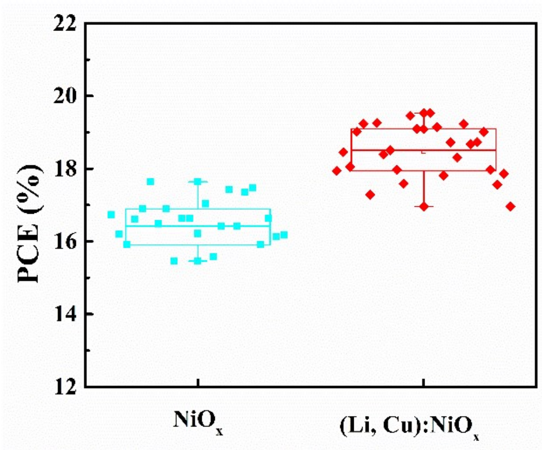

Fig. S7 PCE histogram of 30 pristine NiO_x and (Li, Cu):NiO_x based PSC devices.

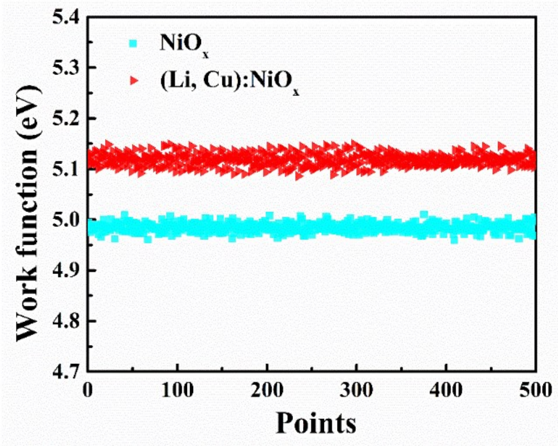

Fig. S8 Work function of (Li, Cu):NiO_x HTL from Kelven Probe.

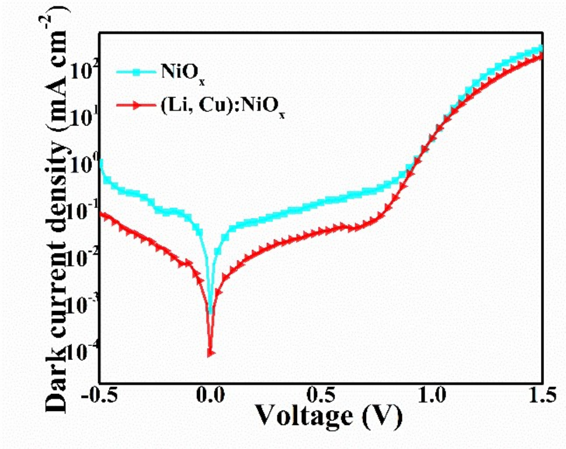

Fig. S9 The dark *J-V* curves of the best-inverted PSCs based on pristine NiO_x and (Li,Cu):NiO_x.

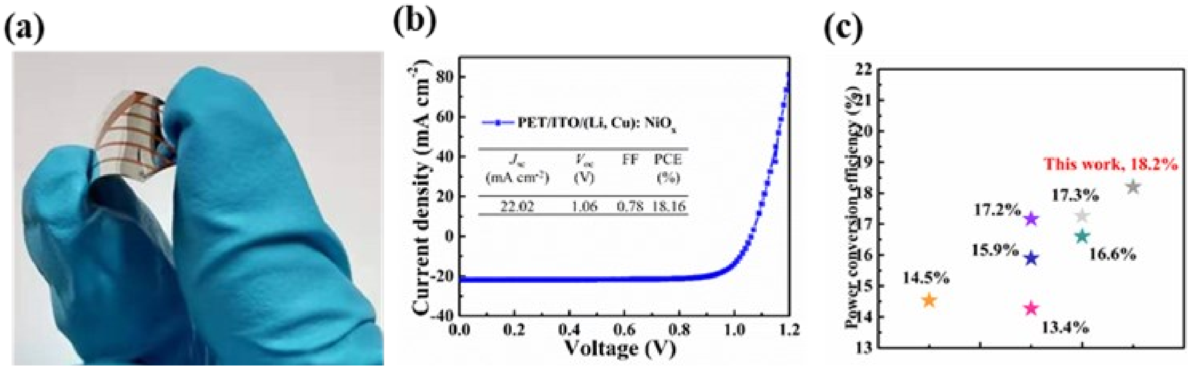

Fig. S10 (a) Photograph of a typical flexible PSC. (b) J-V characterization of (Li,Cu):NiO_x HTL based flexible device. (c) The efficiency of reported NiO_x based flexible devices.

Table S1 Performance of the reported planar PSCs based on NiO_x and doped NiO_x film.

Device Architecture	V_{oc} (V)	J_{sc} (mA cm^{-2})	FF	PCE (%)	Method	Ref.
FTO/NiO_x/$Cs_{0.05}(MA_{0.17}FA_{0.83})_{0.95}Pb(I_{0.9}Br_{0.1})_3$/PCBM/TiOx/Ag	1.10	23.0	0.81	20.65	NPs	1
ITO/NiOx/$MA_{1-y}FA_yPbI_{3-x}Cl_x$/PCBM/BCP/Ag	1.12	23.7	0.76	20.2	Combustion	2
ITO/NiOx/$MAPbI_3$/C_{60}/SnO_2/Ag	1.12	21.8	0.77	18.8	Sol-gel	3
ITO/NiOx/$Cs_{0.05}(MA_{0.17}FA_{0.83})_{0.95}Pb(I_{0.9}Br_{0.1})_3$/PCBM/ZnO/Al	1.02	22.2	0.82	18.6	NPs	4
ITO/NiOx/$MAPbI_3$/PCBM/Ti(Nb)Ox/Ag	1.07	21.9	0.79	18.5	NPs	5
FTO/NiOx/$MAPbI_3$/PCBM/BCP/Ag	1.00	22.9	0.80	18.2	Sol-gel	6
ITO/NiOx/$MAPbI_3$/C60/Bis-C_{60}/Ag	1.03	21.8	0.78	17.7	NPs	7
ITO/NiOx/$MAPbI_3$/PCBM/Bis-C_{60}/Ag	1.10	21.7	0.75	17.6	Sol-gel	8
ITO/NiOx/$MAPbI_3$/PCBM/BCP/Ag	1.02	21.8	0.79	17.6	Spray pyrolysis	9
ITO/PLD-NiOx/$MAPbI_3$/PCBM/LiF/Ag	1.06	20.2	0.81	17.3	PLD	10
ITO/NiOx/$MAPbI_3$/PCBM/Ag	1.04	22.5	0.72	16.9	Electrodeposited	11
ITO/NiOx/$MAPbI_3$/PCBM/Ag	1.07	20.6	0.75	16.5	NPs	12
ITO/NiOx/$MAPbI_3$/PCBM/Ag	1.04	21.9	0.72	16.4	ALD	13
ITO/NiOx/$MAPbI_3$/PCBM/BCP/Ag	0.98	19.7	0.64	12.4	Sputtering	14
ITO/Cu:NiO_x/$MAPbI_3$/PCBM/C_{60}/Ag	1.12	22.2	0.81	20.1	NPs	15
ITO/Zn:NiO_x/$MAPbI_3$/PCBM/C_{60}/Ag	1.10	22.8	0.78	19.6	Sol-gel	16
FTO/Sr:NiOx/$MAPbI_3$/PCBM/BCP/Ag	1.14	22.7	0.76	19.5	Sol-gel	17
FTO/Cs:NiO_x/$MAPbI_3$/PCBM/Zracac/Ag	1.12	21.8	0.79	19.4	Sol-gel	18
FTO/Ca:NiOx/$MAPbI_3$/PCBM/BCP/Ag	1.13	22.3	0.74	18.7	Sol-gel	17
FTO/Mg:NiOx/$MAPbI_3$/PCBM/BCP/Ag	1.10	22.4	0.75	18.3	Sol-gel	17
ITO/K:NiO_x/$MAPbI_3$/PCBM:C_{60}/BCP/Ag	1.01	22.8	0.78	18.1	Sol-gel	19
FTO/Li:NiO_x/$MAPbI_3$/PCBM/Al	1.03	19.4	0.72	14.2	Sol-gel	20
ITO/Cu:NiOx/$MAPbI_3$/C_{60}/Bis-C_{60}/Ag	1.05	22.2	0.76	17.7	Combustion	21
ITO/Ag:NiO_x/$MAPbI_3$/PCBM/C_{60}/Ag	1.09	21.1	0.78	17.3	Sol-gel	22
ITO/Cs:NiO_x/$MAPbI_3$/PCBM/C_{60}/Au	1.03	21.4	0.78	17.2	Sol-gel	23
ITO/Rb:NiOx/$MAPbI_3$/PCBM/BCP/Ag	1.05	21.8	0.75	17.2	Sol-gel	24
ITO/Cu:NiOx/$MAPbI_3$/C_{60}/Bis-C_{60}/Ag	1.11	19.1	0.72	15.4	Sol-gel	25
FTO/La:NiOx/$MAPbI_3$/PCBM/BCP/Ag	1.03	20.7	0.71	15.3	Sol-gel	26
ITO/Co:NiOx/$MAPbI_3$/PCBM/BCP/Ag	1.06	17.3	0.79	14.5	NPs	27
ITO/Li,Ag:NiOx/$MAPbI_3$/PCBM/BCP/Ag	1.13	21.3	0.80	19.2	Sol-gel, 300 °C	28
FTO/$Li_{0.05}Mg_{0.15}Ni_{0.8}O_x$/Psk/Ti(Nb)$O_x$/Ag	1.12	22.7	0.77	19.6	Spray pyrolysis, 500 °C	29
ITO/Li,Pb:NiOx/$MAPbI_3$/PCBM/BCP/Ag	1.01	21.3	0.79	17.4	Sol-gel, 450 °C	30
ITO/Li,Cu:NiOx/$MAPbI_3$/PCBM/Ag	0.96	20.8	0.72	14.5	Sol-gel, 500 °C	31
ITO/(Li,Cu):NiO_x/$MAPbI_{3-x}Cl_x$/PCBM:C_{60}/Zracac/Ag	**1.11**	**23.1**	**0.81**	**20.8**	**NPs, 25 °C**	**this work**

Table S2 The WF variation of pristine NiO_x and doped NiO_x film characterized by Kelvin-Probe measurements. ΔEF is defined as the energy level offsets of the doped film and pristine film.

Material	WF (eV)	ΔE_F (eV)
NiO_x	4.99±0.01	0
Li:NiO_x	5.07±0.0	0.08
(Li, Cu):NiO_x	5.12±0.0	0.13
Cu:NiO_x	5.02±0.0	0.03

Table S3 Summary of device performance with (Li,Cu):NiO_x HTL treated at varying temperatures. The best PCEs are shown in brackets.

Samples	V_{oc} (V)	J_{sc} (mA cm^{-2})	FF	PCE (%)
RT	1.08	22.61	0.78	19.01(20.83)
100 ^oC	1.05	21.88	0.80	18.36(18.63)
150 ^oC	1.04	21.96	0.80	18.30(18.52)
200 ^oC	1.04	21.95	0.81	18.49(18.67)
250 ^oC	1.04	22.12	0.81	18.64(19.00)
300 ^oC	1.02	21.99	0.81	17.99(18.60)

Table S4 Devices performance based on NiO_x HTL with different doping elements.

Doping element	Scan direction	J_{SC} (mA cm^{-2})	V_{OC} (V)	FF	PCE (%)
N/A	Forward	22.02	1.09	0.75	17.91
	Reverse	21.45	1.07	0.73	16.75
Li	Forward	22.69	1.08	0.71	17.49
	Reverse	22.46	1.07	0.71	17.10
(Li, Cu)	Forward	23.07	1.09	0.80	20.08
	Reverse	22.84	1.10	0.80	20.07
Cu	Forward	22.54	1.05	0.75	17.76
	Reverse	21.67	1.03	0.66	14.89

Table S5 Devices performance based on (Li,Cu):NiO_x HTL with different doping concentrations.

Total doping concentration (%)	Ratio of Li/Cu	Scan direction	J_{SC} (mA cm^{-2})	V_{OC} (V)	FF	PCE (%)
0	0	Forward	22.02	1.09	0.75	17.91
		Reverse	21.45	1.07	0.73	16.75
5	2/1	Forward	23.07	1.09	0.80	20.08
		Reverse	22.84	1.10	0.80	20.07
10	2/1	Forward	22.23	1.05	0.74	17.37
		Reverse	21.84	1.03	0.71	16.14
20	2/1	Forward	16.55	1.01	0.72	12.00
		Reverse	15.58	0.99	0.60	9.19

Reference

1 Y. Zhao, H. Zhang, X. Ren, H. L. Zhu, Z. Huang, F. Ye, D. Ouyang, K. W. Cheah, A. K. Y. Jen and W. C. H. Choy, *ACS Energy Lett.*, 2018, **3**, 2891-2898.

2 Z. Liu, J. Chang, Z. Lin, L. Zhou, Z. Yang, D. Chen, C. Zhang, S. F. Liu and Y. Hao, *Adv. Energy Mater.*, 2018, **8**, 1703432.

3 Z. Zhu, Y. Bai, X. Liu, C. C. Chueh, S. Yang and A. K. Jen, *Adv. Mater.*, 2016, **28**, 6478-6484.

4 M. Najafi, F. Di Giacomo, D. Zhang, S. Shanmugam, A. Senes, W. Verhees, A. Hadipour, Y. Galagan, T. Aernouts, S. Veenstra and R. Andriessen, *Small*, 2018, **14**, e1702775.

5 J. He, E. Bi, W. Tang, Y. Wang, Z. Zhou, X. Yang, H. Chen and L. Han, *Solar RRL*, 2018, **2**, 1800004.

6 X. C. Li Juan Tang, Tian Yu Wen, Shuang Yang, Jun Jie Zhao, Hong Wei Qiao, Yu Hou, Hua Gui Yang, *Chem. Eur. J.*, 2018, **24**, 2845-2849.

7 H. Zhang, J. Cheng, F. Lin, H. He, J. Mao, K. S. Wong, A. K. Jen and W. C. Choy, *ACS Nano*, 2016, **10**, 1503-1511.

8 S. Xiao, Y. Bai, X. Meng, T. Zhang, H. Chen, X. Zheng, C. Hu, Y. Qu and S. Yang, *Adv. Funct. Mater.*, 2017, **27**, 1604944.

9 F. Ye, H. Chen, F. Xie, W. Tang, M. Yin, J. He, E. Bi, Y. Wang, X. Yang and L. Han, *Energy Environ. Sci.*, 2016, **9**, 2295-2301.

10 J. H. Park, J. Seo, S. Park, S. S. Shin, Y. C. Kim, N. J. Jeon, H. W. Shin, T. K. Ahn, J. H. Noh, S. C. Yoon, C. S. Hwang and S. I. Seok, *Adv. Mater.*, 2015, **27**, 4013-4019.
11 I. J. Park, G. Kang, A. P. Min, S. K. Ju and Y. K. Jin, *Chemsuschem*, 2017, **10**.
12 X. Yin, P. Chen, M. Que, Y. Xing, W. Que, C. Niu and J. Shao, *ACS Nano*, 2016, **10**, 3630-3636.
13 S. Seo, I. J. Park, M. Kim, S. Lee, C. Bae, H. S. Jung, N. G. Park, J. Y. Kim and H. Shin, *Nanoscale*, 2016, **8**, 11403-11412.
14 H. Lee, Y. T. Huang, M. W. Horn and S. P. Feng, *Sci. Rep.*, 2018, **8**, 5590.
15 W. Chen, Y. Wu, J. Fan, A. B. Djurišić, F. Liu, H. W. Tam, A. Ng, C. Surya, W. K. Chan, D. Wang and Z.-B. He, *Adv. Energy Mater.*, 2018, **8**, 1703519.
16 X. Wan, Y. Jiang, Z. Qiu, H. Zhang, X. Zhu, I. Sikandar, X. Liu, X. Chen and B. Cao, *ACS Appl. Energy Mater.*, 2018, **1**, 3947-3954.
17 B. Ge, H. W. Qiao, Z. Q. Lin, Z. R. Zhou, A. P. Chen, S. Yang, Y. Hou and H. G. Yang, *Solar RRL*, 2019, **3**, 1900192.
18 W. Chen, F.-Z. Liu, X.-Y. Feng, A. B. Djurišić, W. K. Chan and Z.-B. He, *Adv. Energy Mater.*, 2017, **7**, 1700722.
19 X. Yin, J. Han, Y. Zhou, Y. Gu, M. Tai, H. Nan, Y. Zhou, J. Li and H. Lin, *J. Mater. Chem. A*, 2019, **7**, 5666-5676.
20 Z. Saki, K. Sveinbjornsson, G. Boschloo and N. Taghavinia, *Chemphyschem*, 2019, **20**, 3322-3327.
21 J. W. Jung, C. C. Chueh and A. K. Jen, *Adv. Mater.*, 2015, **27**, 7874-7880.
22 J. Zheng, L. Hu, J. S. Yun, M. Zhang, C. F. J. Lau, J. Bing, X. Deng, Q. Ma, Y. Cho, W. Fu, C. Chen, M. A. Green, S. Huang and A. W. Y. Ho-Baillie, *ACS Appl. Energy Mater.*, 2018, **1**, 561-570.
23 H. S. Kim, J. Y. Seo, H. Xie, M. Lira-Cantu, S. M. Zakeeruddin, M. Gratzel and A. Hagfeldt, *ACS Omega*, 2017, **2**, 9074-9079.
24 Q. Fu, S. Xiao, X. Tang and T. Hu, *Org. Electron.*, 2019, **69**, 34-41.
25 J. H. Kim, P. W. Liang, S. T. Williams, N. Cho, C. C. Chueh, M. S. Glaz, D. S. Ginger and A. K. Jen, *Adv. Mater.*, 2015, **27**, 695-701.
26 S. Teo, Z. Guo, Z. Xu, C. Zhang, Y. Kamata, S. Hayase and T. Ma, *ChemSusChem*, 2019, **12**, 518-526.
27 R. Kaneko, T. H. Chowdhury, G. Wu, M. E. Kayesh, S. Kazaoui, K. Sugawa, J.-J. Lee, T. Noda, A. Islam and J. Otsuki, *Solar Energy*, 2019, **181**, 243-250.
28 X. Xia, Y. Jiang, Q. Wan, X. Wang, L. Wang and F. Li, *ACS Appl. Mater. Interfaces*, 2018, **10**, 44501-44510.
29 W. Chen, Y. Wu, Y. Yue, J. Liu, W. Zhang, X. Yang, H. Chen, E. Bi, I. Ashraful, M. Gratzel and L. Han, *Science*, 2015, **350**, 944-948.
30 D. Hou, J. Zhang, X. Gan, H. Yuan, L. Yu, C. Lu, H. Sun, Z. Hu and Y. Zhu, *J. Colloid Interface Sci.*, 2020, **559**, 29-38.
31 M. H. Liu, Z. J. Zhou, P. P. Zhang, Q. W. Tian, W. H. Zhou, D. X. Kou and S. X. Wu, *Opt. Express*, 2016, **24**, A1349-A1359.